

Graphene Converted from the Photoresist Material on Polycrystalline Nickel Substrate

Hyonik Lee, Seulah Lee, Juree Hong, Sang Geun Lee, Jae-Hong Lee, and Taeyoon Lee*

Nanobio Device Laboratory, School of Electrical and Electronic Engineering, Yonsei University, Seoul 120-749, Korea

Received December 1, 2011; accepted March 25, 2012; published online June 20, 2012

Graphene has attracted attention from both academia and industry owing to its fascinating properties and a wide range of potential applications. Methods for graphene synthesis from solid and liquid carbon sources, including poly(methyl methacrylate) (PMMA), benzene, and other carbon sources, have been reported due to the potential use of a wide variety of carbon feedstocks. In this study, high quality graphene was grown from SU-8-2002 photoresist materials on Ni foil with annealing at 1000 °C for 20 min in an ambient mixture of He and H₂ gas. Scanning electron microscopy image of the as-synthesized graphene on Ni foil indicated that graphene covered the whole area of the Ni foil with various numbers of layers due to the different carbon segregation rate depending on the underlying Ni grain orientation. To unambiguously distinguish the thickness variation of the synthesized graphene layers, they were transferred onto SiO₂ (300 nm)/Si substrate and were analyzed using optical microscopy, and Raman spectroscopy, which confirmed that the synthesized graphene is composed of various numbers of layers. The thickness dependent G/2D peak intensity ratio (I_G/I_{2D}) of Raman spectra and their full width at half maximum values obtained from the transferred graphene layers were examined, which were in good accordance with atomic force microscopy analyses. © 2012 The Japan Society of Applied Physics

1. Introduction

Graphene, which is the monolayer form of carbon atoms arranged in two-dimensional (2D) hexagonal lattices, has attracted widespread interests owing to its outstanding electronic and mechanical properties.¹⁻⁴ In past years, most research efforts have been devoted to graphene synthesis methods such as mechanical exfoliation,¹ epitaxial synthesis on SiC,⁵ liquid phase exfoliation,⁶ and chemical vapor deposition (CVD) methods.⁷ Among them, especially the CVD method, which is used for graphene growth through the catalytic decomposition of hydrocarbon gas sources on transition metal substrates (such as Cu and Ni), is a promising technique for the mass production of high quality graphene at a relatively low cost.^{7,8}

However, the CVD method is not applicable to a variety of feedstocks as it is limited to gas-phase carbon source such as CH₄, and C₂H₂.⁹ Recent studies in graphene synthesis, suggest that various carbon solid or liquid sources such as poly(methyl methacrylate) (PMMA),^{9,10} benzene and even food and insects¹¹ can be used to grow high-quality monolayer graphene on Cu foils with an annealing process. The growth of graphene using different carbon solid or liquid sources has several merits including a relatively low fabrication temperature, environmentally friendly process, and potential application to mass-production. Moreover, methods that can be used to grow graphene from diverse carbon sources can provide an opportunity to understand the growth mechanism of graphene itself.

In this study, graphene was successfully grown using an SU-8-2002 photoresist (PR) material as a solid carbon source spin-coated on a Ni foil with a subsequent annealing process at 1000 °C and natural cooling to room temperature. Bright contrast in the scanning electron microscopy (SEM) image was observed from the as-synthesized graphene on Ni foil, indicating that graphene covered the whole area of the Ni foil. The extremely low intensity of the D peak ($\sim 1350 \text{ cm}^{-1}$) in Raman spectra before transfer procedure, confirmed that the synthesized graphene was almost defect-free, except for the ripple-structured sites in the thicker layer graphene. We confirmed that the transferred graphene on SiO₂ (300 nm)/Si substrate is consisted of various layers

from mono- to multi-layers using a combination of Raman spectroscopy and atomic force microscopy (AFM) measurements. The representative G/2D peak intensity ratio (I_G/I_{2D}) of Raman spectra was approximately: 0.3 for mono-layer graphene, 1.4 for few-layered graphene, and 1.9 for multi-layered graphene. The existence of D peak in the Raman spectrum of the transferred graphene, mainly in mono-layered regions, can be explained by the higher chance of structural deformation during the transfer procedure, while the disappearance of the D peak in thicker-layered regions may be ascribed to a flattening phenomenon during the transfer procedure. Compared with previously reported graphene synthesis on Cu and Ni foil using the CVD method the graphene obtained from this experiment consisted of various layers of graphene due to the segregation and precipitation mechanisms of graphene growth on the Ni foil.^{12,13}

2. Experimental Procedure

The 25- μm -thick, 99.5% metal basis annealed Ni foil (Alfa Aesar 00228) with $1 \times 1 \text{ cm}^2$ size was cleaned by successive ultrasonication in acetone, ethanol, and de-ionized (DI) water for 5 min each. A volume of 500 μL SU-8-2002 PR material [MicroChem SU-8-2002, 29% in cyclopentanone (C₅H₈O), including mixed triarylsulfonium [C₃₆H₂₈S₃ · 2(SbF₆)], propylene carbonate (C₄H₆O₃)], and epoxy resin (C₁₉H₂₃ClO₄) was deposited on the cleaned-Ni foil by spin coating at 5000 rpm for 30 s. The obtained SU-8-2002/Ni foil sample was cured at 110 °C for 1 min. The prepared sample was loaded into a CVD quartz chamber. The chamber was maintained at a total pressure of 2.7 Torr with 500 sccm H₂ and 1000 sccm He gas flow and heated to 1000 °C. The ramping rate was approximately 30 °C/min during the heating procedure. The sample was annealed at 1000 °C for 20 min and naturally cooled down to room temperature while maintaining a gas configuration identical to the annealing conditions. The synthesized graphene/Ni foil sample was observed by SEM (JEOL JSM-600F). To investigate the thickness of the synthesized graphene, the SU-8-2002 derived graphene was transferred onto a SiO₂ (300 nm)/Si substrate by the following procedure; PMMA was spin coated onto the surface of the graphene film to serve as a support. The PMMA/graphene/Ni foil layer was dipped into a 3 wt % aqueous solution of hydrochloric acid

*E-mail address: taeyoon.lee@yonsei.ac.kr

to etch the Ni foil. The resulting PMMA/graphene sample was manually laid on the SiO₂ (300 nm)/Si substrate. The PMMA was finally removed by an acetone solution. The prepared sample was investigated by optical microscopy accompanied red green blue (RGB) contrast image analysis using Adobe Photoshop CS5. The thickness of the transferred graphene was quantified by XE-100 AFM of Park System in which the scans of several 25 × 25 μm² area are obtained, along with the use of large surface, high magnification, non-contact white light interferometer of the Zygo's New View 6300 System. An X-ray diffractometer (XRD) equipped with a Ni-filtered K α ($\lambda = 1.54056 \text{ \AA}$) source was used for structural analysis of the Ni foil before and after annealing. Raman spectra were obtained using a micro-Raman system (Jobin-Yvon LabRam HR) with a 514.532 nm Ar-ion laser to characterize the SU-8-2002 PR derived graphene on Ni foil.

3. Results and Discussion

Figure 1(a) shows a schematic illustration of the graphene synthesis process using SU-8-2002 as a solid carbon source. The PR coated-Ni foil was heated up to 1000 °C and annealed with the mixture of He and H₂ gas ambient. The catalytically decomposed carbon atoms from the solid carbon sources may diffuse into the Ni foil during the annealing process due to the relatively high solubility of carbon in the Ni foil (2.7% at 1455 °C).^{13–15} Graphene synthesis on the Ni substrate is known to be governed by segregation or precipitation of the decomposed carbon sources during the cooling process.¹⁶ To be specific, the solubility of the carbon source decreases during cooling, which cause the excess carbon atoms to become out-diffused on the Ni surface, thus very thin graphene sheets are formed on the surface of Ni substrate. Figure 1(b) shows an SEM image of the SU-8-2002 PR derived graphene on Ni foil. Based upon the bright contrast of the SEM images from the grown graphene layers, it was clear that thicker and thinner-layered graphene coexisted with no ordering; the dark areas represent thicker layers, and the light areas represent thinner graphene. The dotted lines indicate the grain boundaries of Ni and they were perfectly matched with the bright contrast of the SEM image. The formation of regions with a different number of graphene layers may originate from the different crystalline orientations of the polycrystalline Ni grains. These varied grain orientations yield different carbon atom diffusion rates along the direction perpendicular to the surface of the grain during segregation or precipitation in the cooling process. The surface self-diffusion parameter of the direction perpendicular to the (111) plane of Ni is $1.9 \times 10^{-3} \text{ cm}^2/\text{s}$ and that of the (100) plane is $2.1 \text{ cm}^2/\text{s}$.¹⁷ Thus, a larger amount of segregated C atoms on the Ni(100) grain surface can be expected, which then leads, to the formation of thicker-layered graphene. In contrast, the smaller number of C atoms provided from the (111) Ni grain could form a thinner layer of graphene, which was found to be monolayer graphene by Raman analysis. Similar results were found^{18,19} with respect to the correlation between orientation and the number of graphene layers when gas sources were used for synthesis. Specifically, Zhang *et al.* reported a preferential formation of monolayer/bilayer graphene with respect to the different crystalline orientations of Ni grains.¹⁹

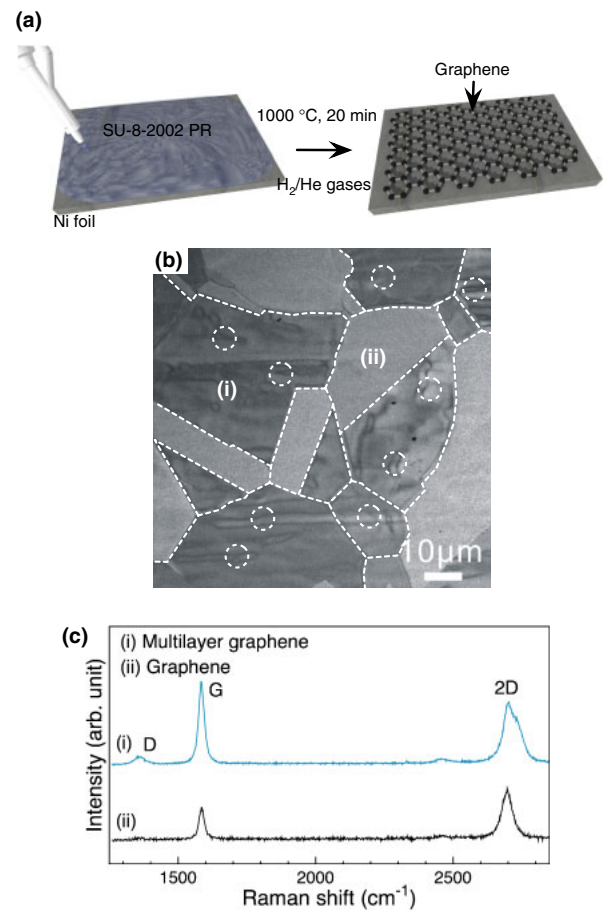


Fig. 1. (Color online) Synthetic protocol, SEM image of SU-8-2002 derived graphene, and its Raman spectrum; (a) Synthetic schematic of graphene from an SU-8-2002 photoresist material coated on a nickel foil. (b) SEM image of SU-8-2002-derived graphene on nickel foil. The dotted lines and circles indicate the Ni grain boundary and wrinkles, respectively. The region denoted as (i) corresponds to the region covered with thicker graphene layers as compared to region (ii). (c) Comparison of graphene Raman spectra in regions (i) and (ii).

Interestingly, most of the ripple structures were observed in thicker graphene region as indicated by the dotted circles in Fig. 1(b). Once the initial graphene islands form, they grow in size independently and come in to contact with adjacent graphene grains. Intense stress may be incorporated toward the grain center in regions where graphene grains join. In addition, due to the large differential thermal contraction coefficient between graphene and Ni, a large compressive stress would be incorporated in graphene layers during the cooling process. The thermal expansion coefficient (TEC) of Ni is $3.4 \times 10^{-6} \text{ K}^{-1}$.²⁰ Notably, the graphene shows an extraordinary in-plane negative TEC of $-6 \times 10^{-6} \text{ K}^{-1}$.¹⁵ Thus, ripple formation cannot be avoided in this synthesis process. Since the TEC would differ due to the orientation of Ni grains, differing in-plane contractions of the graphene layer on the corresponding underlying Ni grain can be expected. However, the distinct disparity in the population of the ripple structure between the thicker- and thinner-layered of graphene can be primarily attributed to the higher diffusivity of C atoms on the (100) Ni grain compared with that on the (111) Ni grain. Wrinkle formation in the graphene layers on a polycrystalline Ni substrate was investigated by Chae *et al.*

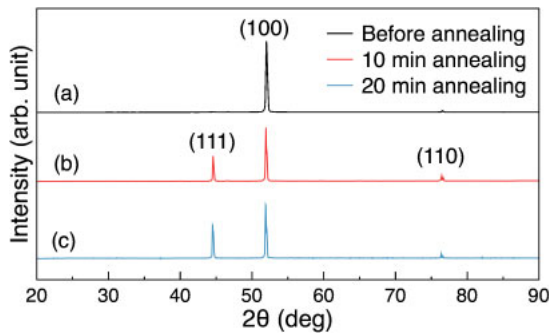


Fig. 2. (Color online) XRD θ - 2θ scans obtained from (a) as-treated and those annealed for (b) 10, and 20 min.

using CVD process.²¹⁾ They found that the wrinkle height increases with respect to growth time mainly due to the higher probability of having more wrinkles in thicker graphene layers. Within the same cooling time in our experiment, the amount of C employed in the formation of graphene on the Ni grain with the higher carbon diffusivity was larger, thus the number of graphene sheets and the probability of wrinkle formation could be higher. The wrinkle-induced defective graphene structure was confirmed by Raman spectroscopy analysis of the synthesized graphene on Ni foil. Figure 1(c) shows Raman spectra obtained from the thicker and thinner layers of graphene denoted as (i) and (ii), respectively, in Fig. 1(b). Raman spectra for region (i) exhibited small peaks near 1350 cm^{-1} , which indicated defective graphite and are referred to as disorder induced D bands,²²⁾ while no D-bands were seen in region (ii). Such small D peaks can be attributed to the existence of ripples in region (i). Wrinkles were rarely observed in the thinner graphene regions, which is consistent with the observation that there is no D-band peak in the Raman spectrum of region (ii).

XRD analyses were performed to investigate the effect of the annealing process on the crystalline orientation of the Ni foil and the resulting spectra are shown in Fig. 2. Since Ni(100) single-crystalline foil was used, a sole prominent (100) peak was observed prior to annealing in the XRD spectra over the 2θ range 20 – 90° , as shown in Fig. 2(a). The peak centered at 51.9° ²³⁾ is the Ni(100) peak and its full width at half maximum (FWHM, $\Gamma_{2\theta}$) intensity value is $\Gamma_{2\theta} = 0.4^\circ$. A very tiny (110) peak was observed at 76.4° , but its intensity was small enough to be negligible. Figures 2(b) and 2(c) exhibit the XRD spectrum of the Ni foils after 10 and 20 min annealing, respectively. Compared with Fig. 2(a), the XRD spectra obtained after annealing has a (111) peak at 44.5° and (110) peak at 76.4° ,²³⁾ indicating that the predominant (100) crystalline orientation prior to annealing was partially transformed into the (111) crystal direction after annealing fabrication. The peak centered at 51.9° is the Ni(111) peak and the intensity of this peak gradually increased with annealing time. The preferential crystalline orientation of Ni(111) can be confirmed from the texture coefficient (TC), which can be derived as

$$TC = \frac{I_{(111)}}{I_{(111)} + I_{(100)} + I_{(110)}}, \quad (1)$$

where $I_{(111)}$, $I_{(100)}$, and $I_{(110)}$ are the integrated intensities of the (111), (100), and (110) planes, respectively. The calculated TC in samples exceeded 0.30 after 10 min of annealing and 0.34 after 20 min of annealing at 1000°C . The higher value of the calculated TC indicated that the proportion of the (111) Ni grains increased with annealing time. In face centered cubic (fcc) metals including Ni, the (111) planes always have the lowest surface/interface energy with respect to other crystallographic orientations.²⁴⁾ These XRD results are consistent with the prior discussion related to Fig. 1(b). During the annealing process, the Ni foil was transformed into poly-Ni. A variation in the thickness of the graphene layer occurred due to the differential diffusivity of C with respect to the orientation of Ni.

To verify the exact thickness variation of the synthesized graphene layers derived from SU-8-2002, they were transferred onto a 300-nm-thick SiO_2 substrate and were analyzed using optical, Raman, and AFM tools, as such measurements were inadequate to take on a Ni foil owing to the superimposition of the graphene layers on Ni grains.²⁵⁾ It has been previously reported by Wang *et al.* that the Raman features are affected by the interaction between the support substrate and graphene sheets.²⁵⁾ In order to carry out an accurate Raman spectroscopy and AFM analyses to circumvent the effect of Ni substrate, the substrate supporting the graphene layers needs to be non-metal. Figure 3(a) shows an optical micrograph of graphene transferred onto 300-nm-thick SiO_2 , and its corresponding RGB contrast image is illustrated in Fig. 3(b). Ni *et al.* discriminated the thickness of graphene on SiO_2 (285 nm)/Si substrate using color contrast spectra, which were generated from the reflection light of a white light source.²⁶⁾ Although the observation of optical micrograph for the graphene sheets of different thickness cannot provide quantitative information due to the fact that it varies from one laboratory to another and it relies on experience of the observer and the experimental setup of optical microscope, it is still meaningful to determine the relative thickness variation of the obtained graphene layers roughly within a single reflection color contrast optical image. The purpose of illustrating the RGB color contrast contour map was to more visualize the distribution of thickness variation of the transferred graphene layers, combined with other measurements, which will be discussed later. The color contrast of optical micrographs was enhanced by RGB expression, as shown in Fig. 3(b).²⁷⁾ The red, green, and blue color contrast regions in Fig. 3(b) take up approximately 48, 13, and 39% of the whole image, respectively.

Figure 3(c) illustrates 15 typical Raman spectra measured along the dotted-line drawn on Fig. 3(b), which includes all three pronounced color contrast of green, red, and blue. Here, the peaks located at ~ 1590 and $\sim 2700\text{ cm}^{-1}$ are assigned as G and 2D bands, respectively. The 15 typical Raman spectra in Fig. 3(c) can be classified into three groups according to the value of I_G/I_{2D} and FWHM, as shown in Fig. 3(d). The first group of the spectra is similar to the spectra of mono-layered graphene, which have narrow line widths for 2D bands ($\sim 40\text{ cm}^{-1}$), and $I_G/I_{2D} < 0.75$. On the other hand, the second group of spectra has an apparent broadening of 2D band line widths ($\sim 65\text{ cm}^{-1}$). Moreover, I_G/I_{2D} for the second group of Raman spectra is

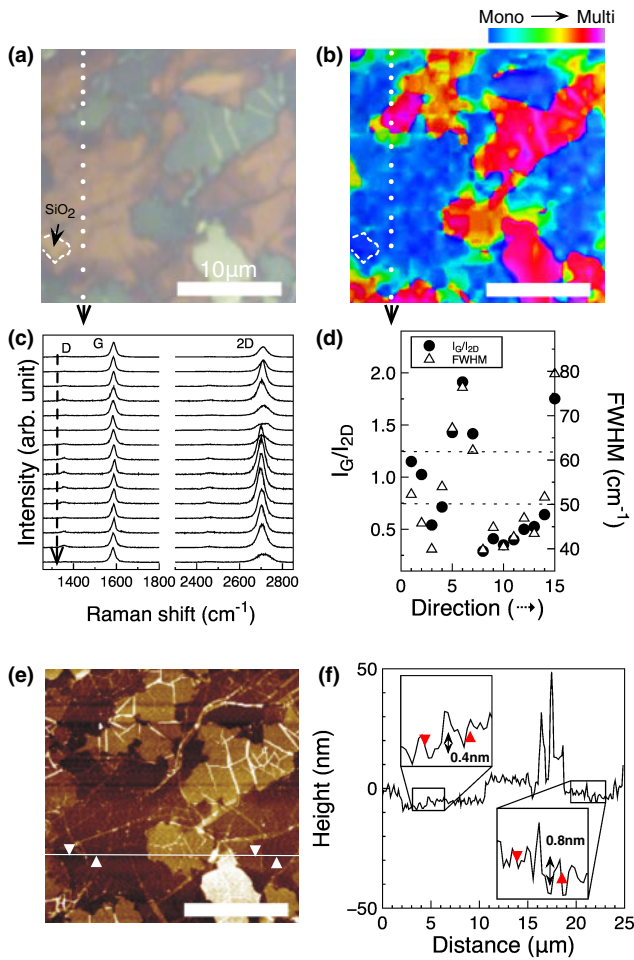


Fig. 3. (Color online) Analysis of graphene transferred on SiO₂ (300 nm)/Si substrate; (a) Optical micrograph of graphene transferred on SiO₂ (300 nm)/Si. (b) Respective color contrast image of (a). (c) Raman spectra obtained along the white dotted-line drawn on (a). The dots indicate the actual measured spots. (d) I_G/I_{2D} and FWHM of 2D bands obtained from (c). (e) AFM image taken from the same area in (a). (f) Height profile along the horizontal line drawn on (e).

around 1, which is the characteristic of few-layered graphene.^{26,28} Lastly, the third group of spectra shows a further broadening of 2D band ($\sim 80 \text{ cm}^{-1}$) and their I_G/I_{2D} nearing 2, indicating that they are multi-layered graphene. The I_G/I_{2D} , FWHM of 2D bands, and the transparency of transferred graphene layers in optical micrograph are in good accordance with the results of previous report.²⁶ Interestingly, Raman spectra obtained from the first group exhibited small D peaks ($\sim 1350 \text{ cm}^{-1}$),²² whereas no significant D peak was observed from the third group. This result is the opposite of that obtained before the transfer process, and it can be explained by the different deformation mechanism of the graphene layers during the transfer process. The D peaks found in the first group after the transfer process may be originated from the higher chance of distortion introduced during the transfer process owing to their extremely thin thickness, while the D peaks in the third group has been reduced since they are subject to less deformation or even flattening due to their thicker nature.²⁹ Zhang *et al.* reported that depending on the graphene-substrate adhesion, number of graphene layers, and substrate stiffness, graphene layers exhibit different types of morphol-

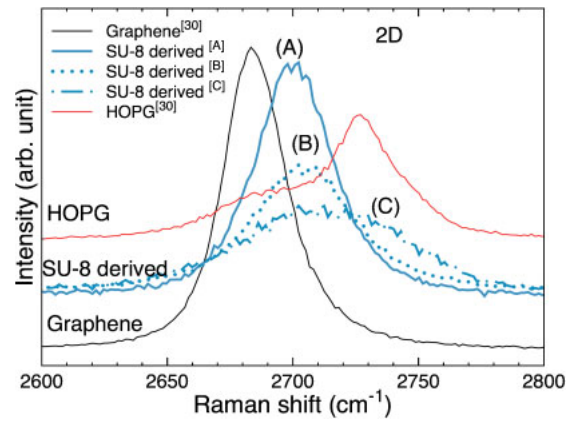


Fig. 4. (Color online) Raman spectra of 2D bands from representative SU-8-2002-derived mono-, few-, and multi-layered graphene, HOPG, and pristine graphene. The data for the pristine graphene and HOPG were extracted from the work of Ferrari *et al.*³⁰ The solid line (A) corresponds to the Raman spectra of mono-layered graphene; the dotted-line (B) corresponds to the Raman spectra of few-layered graphene; and the dash-dotted line (C) corresponds to the Raman spectra of multi-layered graphene.

ogy after they have been transferred. Figure 3(e) corresponds to the AFM image of the same region as Fig. 3(a), and Fig. 3(f) shows the height profile analyzed along the white line drawn in Fig. 3(e). The height difference between the arrows set in the left side of Fig. 3(e) (from the SiO₂ to graphene sheet) was $\sim 0.4 \text{ nm}$, which can be considered as mono-layered graphene. The height difference between the arrows set at the right side of the image was $\sim 0.8 \text{ nm}$ which corresponds to two layers of graphene. The thickness of multi-layered graphene was approximately 15 nm, which correspond to few tens of layers of graphene.

The number of graphene layers can also be confirmed by the peak position of the 2D band. Ferrari *et al.*³⁰ reported that the peak position of the 2D-band (at $\sim 2690 \text{ cm}^{-1}$) shows an up-shifted pattern as the number of layers increases, while the G-band (at $\sim 1580 \text{ cm}^{-1}$) is unchanged. Thus, an accurate peak position of Raman shift for the SU-8-2002-derived graphene is worth comparing to those of pristine graphene and highly oriented pyrolytic graphite (HOPG). Figure 4 shows Raman spectra obtained from the synthesized graphene, the corresponding areas of which are representative of mono-, few-, and multi-layered graphene. The Raman spectra for HOPG and pristine graphene in Fig. 4 are extracted from.³⁰ The peak located around 2683 cm^{-1} is assigned as the 2D band of the graphene layer. The 2D peaks of pristine graphene, SU-8-2002 derived mono-, few-, and multi-layered graphene and HOPG, which appear at around 2683, 2697, 2702, 2722, and 2729 cm^{-1} , respectively, were gradually up-shifted. The differences in the 2D peak position between pristine graphene and SU-8-2002 derived mono- and multi-layered graphene were approximately 14, 19, and 39 cm^{-1} , respectively, and these values are equivalent to the up-shifted nature of mono-, few-, and multi-layered graphene.³¹ The 2D-band profile also shows asymmetric characteristics with regard to the number of graphene layers, which corroborates a previous report.³¹

4. Conclusions

Here, we demonstrated that thin graphene could be synthesized on Ni foil using SU-8-2002 PR as a solid carbon source via a successive annealing process and cooling procedure in a mixture of He and H₂ gas. The bright contrast in the SEM image confirmed that the whole area of Ni foil was covered by graphene layers with variation in thickness. During the annealing process, the recrystallized polycrystalline Ni foil with (111) and (100) orientations induced differential C diffusion rates according to texture, which resulted in variation in the number of graphene layers. The combination of Raman spectroscopic analyses, optical micrograph, and AFM image with corresponding height profile of the synthesized graphene, transferred onto 300-nm-thick SiO₂/Si substrate, indicated that the synthesized graphene are composed of various numbers of layers. The use of new carbon materials may lead to a new understanding of the mechanism of graphene synthesis.

Acknowledgments

This work was supported by the Korea Aerospace Research Institute (KARI)-University partnership program and by the Entrepreneurship (EP) Program funded by the Korea Institute of Science and Technology (KIST, 2V02230). This research was also supported in part by the Converging Research Center Program through the Ministry of Education, Science and Technology (2011K000631) and by the Priority Research Centers Program through the National Research Foundation of Korea (NRF) funded by the Ministry of Education, Science and Technology (2009-0093823).

- 1) K. Novoselov, A. Geim, S. Morozov, D. Jiang, Y. Zhang, S. Dubonos, I. Grigorieva, and A. Firsov: *Science* **306** (2004) 666.
- 2) A. K. Geim and K. S. Novoselov: *Nat. Mater.* **6** (2007) 183.
- 3) Y. Zhang, Y. W. Tan, H. L. Stormer, and P. Kim: *Nature* **438** (2005) 201.
- 4) R. Ruoff: *Nat. Nanotechnol.* **3** (2008) 10.
- 5) V. W. Brar, Y. Zhang, Y. Yayon, T. Ohta, J. L. McChesney, A. Bostwick,

- E. Rotenberg, K. Horn, and M. F. Crommie: *Appl. Phys. Lett.* **91** (2007) 122102.
- 6) H. C. Schniepp, J. L. Li, M. J. McAllister, H. Sai, M. Herrera-Alonso, D. H. Adamson, R. K. Prud'homme, R. Car, D. A. Saville, and I. A. Aksay: *J. Phys. Chem. B* **110** (2006) 8535.
- 7) X. Li, W. Cai, J. An, S. Kim, J. Nah, D. Yang, R. Piner, A. Velamakanni, I. Jung, and E. Tutuc: *Science* **324** (2009) 1312.
- 8) Y. Lee, S. Bae, H. Jang, S. Jang, S. E. Zhu, S. H. Sim, Y. I. Song, B. H. Hong, and J. H. Ahn: *Nano Lett.* **10** (2010) 490.
- 9) Z. Sun, Z. Yan, J. Yao, E. Beitler, Y. Zhu, and J. M. Tour: *Nature* **25** (2010) 549.
- 10) S. J. Byun, H. Lim, G. Y. Shin, T. H. Han, S. H. Oh, J. H. Ahn, H. C. Choi, and T. W. Lee: *Phys. Chem. Lett.* **2** (2011) 493.
- 11) Z. Li, P. Wu, C. Wang, X. Fan, W. Zhang, X. Zhai, C. Zeng, J. Yang, and J. Hou: *ACS Nano* **5** (2011) 3385.
- 12) R. Negishi, H. Hirano, Y. Ohno, K. Haehashi, K. Matsumoto, and Y. Kobayashi: *Jpn. J. Appl. Phys.* **50** (2011) 06GE04.
- 13) A. Reina, S. Thiele, X. Jia, S. Bhaviripudi, M. S. Dresselhaus, J. A. Schaefer, and J. Kong: *Nano Res.* **2** (2009) 509.
- 14) S. Takenaka, Y. Shigeta, E. Tanabe, and K. Otsuka: *J. Phys. Chem. B* **108** (2004) 7656.
- 15) J. W. Jiang, J. S. Wang, and B. Li: *Phys. Rev. B* **80** (2009) 205429.
- 16) X. Li, W. Cai, L. Colombo, and R. S. Ruoff: *Nano Lett.* **9** (2009) 4268.
- 17) H. Bonzel and E. Latta: *Surf. Sci.* **76** (1978) 275.
- 18) N. Liu, L. Fu, B. Dai, K. Yan, X. Liu, R. Zhao, Y. Zhang, and Z. Liu: *Nano Lett.* **11** (2011) 297.
- 19) Y. Zhang, L. Gomez, F. N. Ishikawa, A. Madaria, K. Ryu, C. Wang, A. Badmaev, and C. Zhou: *Phys. Chem. Lett.* **1** (2010) 3101.
- 20) T. Kollie: *Phys. Rev. B* **16** (1977) 4872.
- 21) S. J. Chae, F. Gune, K. K. Kim, E. S. Kim, G. H. Han, S. M. Kim, H. J. Shin, S. M. Yoon, J. Y. Choi, and M. H. Park: *Adv. Mater.* **21** (2009) 2328.
- 22) C. Casiraghi, A. Hartschuh, H. Qian, S. Piscanec, C. Georgi, A. Fasoli, K. Novoselov, D. Basko, and A. Ferrari: *Nano Lett.* **9** (2009) 1433.
- 23) JCPDS 04-0850.
- 24) R. Carel, C. Thompson, and H. Frost: *Acta Mater.* **44** (1996) 2479.
- 25) Y. Wang, Z. Ni, T. Yu, Z. X. Shen, H. Wang, Y. Wu, W. Chen, and A. T. Shen Wee: *J. Phys. Chem. C* **112** (2008) 10637.
- 26) Z. Ni, H. Wang, J. Kasim, H. Fan, T. Yu, Y. Wu, Y. Feng, and Z. Shen: *Nano Lett.* **7** (2007) 2758.
- 27) J. D. Foley: *Computer Graphics: Principles and Practice* (Addison-Wesley, Reading, MA, 1996).
- 28) A. Reina, X. Jia, J. Ho, D. Nezich, H. Son, V. Bulovic, M. S. Dresselhaus, and J. Kong: *Nano Lett.* **9** (2009) 3087.
- 29) Z. Zhang and T. Li: *J. Appl. Phys.* **110** (2011) 083526.
- 30) A. Ferrari, J. Meyer, V. Scardaci, C. Casiraghi, M. Lazzeri, F. Mauri, S. Piscanec, D. Jiang, K. Novoselov, and S. Roth: *Phys. Rev. Lett.* **97** (2006) 187401.
- 31) B. Tang, H. Guoxin, and H. Gao: *Appl. Spectrosc. Rev.* **45** (2010) 369.